RAPIDLY ADAPTIVE CFAR DETECTION BY MERGING INDIVIDUAL DECISIONS FROM TWO-STAGE ADAPTIVE DETECTORS

Anatolii A. Kononov, Sung-Hyun Choi and Jin-Ha Kim
Research Center, STX Engine
Yongin-si, 16914 Korea
kaa@ieee.org; dkrein@onestx.com; kjinha@onestx.com

Abstract— This paper addresses the problem of target detection in adaptive arrays in situations where only a small number of training samples is available. Within the framework of two-stage adaptive detection paradigm, we propose a new two-stage (TS) joint loaded persymmetric-Toeplitz adaptive matched filter (JLPT-AMF) detector. This new detector combines, using a joint detection strategy, individual scalar CFAR decisions from two rapidly adaptive detectors: a TS TAMF detector and a TS LPAMF detector. The former is based on a TMI filter, which is an adaptive array filter employing a Toeplitz covariance matrix estimator introduced in [1]. The latter is based on an adaptive LPMI filter that uses diagonally loaded persymmetric covariance matrix (CM) estimate inversion. The TS JLPT-AMF detector ensures the constant false alarm rate (CFAR) property independently of the antenna array dimension M, the interference CM, and the number of training samples N_{CME} to be used for estimating this CM. This new detector exhibits highly reliable detection performance, which is robust to the angular separation between the sources, even when N_{CME} is about $m/2 \sim m$, m is the number of interference sources. The robustness of the proposed adaptive detector to the angular separation is analytically proven and verified with statistical simulation.

Keywords— adaptive array; CFAR detection; persymmetry; radar; Toeplitz matrix; two-stage detection

I. INTRODUCTION

The adaptive TMI filters based on the Toeplitz covariance matrix (CM) estimator proposed in [1] exhibit a superfast convergence rate in terms of the 3dB average signal-to-noise ratio loss for the low-rank (LR) covariance scenarios when the exact CM **R** of the interference has a "cliff-like" eigenspectrum

$$\lambda_1 \geq \lambda_2 \geq \ldots \geq \lambda_m >> \lambda_{m+1} = \ldots = \lambda_M = \sigma_o^2, \qquad (1)$$

where λ_k, k = 1, 2, ..., M are the eigenvalues of **R**, M is the array dimension; m is the number of external powerful interference sources ($m \ll M$) and $\sigma_o^2 = p_o$ stands for the additive white Gaussian noise power.

TMI filters require $m/2$ training samples to achieve the 3dB average signal-to-noise ratio (SNR) loss, while the diagonally loaded persymmetric CM estimate inversion (LPMI) filters and the conventional LSMI filters require m and $2m$ samples, respectively. TMI filters can achieve such exceptionally rapid convergence rate if the angular separation between sources does not too closely approach the statistical resolution limit (SRL) defined in [2]. As demonstrated in [1], the convergence performance of the MUSIC-based TMI filters may degrade due to a possible unacceptable drop in output SNR when the angular separation between sources is near the SRL. Though using other direction of arrival (DOA) estimators, such as Root-MUSIC [3] or ESPRIT [4], can make TMI filters less sensitive to the small angular separation between sources, this approach does not provide a reliable remedy because performance breakdown resides in all known DOA estimators.

Also, note that detectors employing the adaptive TMI filters introduced in [1] are not strictly CFAR detectors; loss of the CFAR property is the price paid for achieving the superfast convergence rate.

Basic adaptive detectors (BADs), such as the generalized likelihood ratio test (GRLT), the adaptive matched filter (AMF), and the adaptive coherence estimator (ACE), possess two invariance properties relative to the unknown CM of interference. These are the invariance of the detector's output statistics resulting in the CFAR property of the detector, and the invariance of the detection performance loss compared with the clairvoyant detector.

BADs exhibit these important properties only if the number of training samples significantly exceeds the array dimension [5, 6]. Moreover, BADs possess the strict CFAR property primarily because they use a generic maximum-likelihood (ML) sample CM (SCM) estimator; this estimator ignores any a priori information on the exact CM **R**. Ignoring this information results in the need for a considerable number of training samples to ensure the CFAR property and reliable detection performance.

Table I is based on the results reported in [1]. This table summarizes the ratio q_{RAD} of the total number of real variables (all real and imaginary parts) contained in the complex-valued entries of training data samples, to the total number of free real variables contained in the complex-valued entries of all the signal subspace (dominant) eigenvectors of the exact CM **R** depending on a priori information about **R** incorporated into the CM estimator. The free real variables are all the real and imaginary parts, with no constraints imposed on them, of all complex-valued entries in the dominant eigenvectors.

In Table I, the quantity Q_{TDS} is represented as $Q_{\text{TDS}} = N_{3\text{dB}} \times Q_{\text{ITS}}$, where $N_{3\text{dB}}$ is the minimum number of training samples required to achieve the 3dB average SNR loss relative to the Wiener filter, and Q_{ITS} is the number of real and imaginary parts in one training sample (vector). The quantity

TABLE I. NUMBER OF REAL TRAINING VARIABLES PER ONE FREE REAL VARIABLE DEPENDING ON STRUCTURE OF TRUE CM

Structure of true CM	**Total number of real variables in training data set**, Q_{TDS}	**Total number of free real variables**, Q_{FRV}	q_{RAD}
General	$2M\times 2M$	$M\times 2M$	2
Low-rank (LR)	$2m\times 2M$	$m\times 2M$	2
LR+Persymmetry	$m\times 2M$	$m\times M$	2
LR+Toeplitz	$m/2\times 2M$	$m\times M/2$	2

Q_{FRV} is represented as $Q_{FRV} = N_{DEV}\times Q_{IEV}$, where N_{DEV} is the number of the dominant eigenvectors of $\mathbf{R}$ and Q_{IEV} is the number of free real variables in each dominant eigenvector.

Analysis of the $q_{RAD} = Q_{TDS}/Q_{FRV}$ ratio in Table I leads to the conclusion that the following *condition of reliable adaptive detection is valid (at least for Gaussian interference); q_{RAD} must meet the condition $q_{RAD}>2$ to ensure reliable adaptive detection; in other words, the ratio of the total number of real variables in a training data set to the total number of free real variables in the dominant eigenvectors of the exact CM has to exceed* 2.

This fundamental condition has been verified for general and for low-rank structures of the true CM; rigorous proofs, in terms of the probability density functions for the SNR at the output of adaptive filters, are given in [7] and [8, 9], respectively. The two remaining cases in Table I have not yet been rigorously proven; however, these cases are confirmed by numerous Monte-Carlo simulations.

In many cases, BADs' very attractive features discussed above cannot be used; however, they can be achieved within the framework of a two-stage detection approach [5, 6]. This approach appears to be the only feasible adaptive detection option when the CFAR property cannot be realized even theoretically, e.g., in *non-homogeneous training conditions* that occur due to the statistical discrepancy between the training data and the primary data, see for details [5, 6]. A similar two-stage approach may also be considered for homogeneous training conditions.

In the case of homogeneous training conditions, a set of N independent identically distributed (IID) *training samples* allocated for any single primary range cell is divided into two subsets of the N_{CME} and the N_{CFAR} samples. The former is used in estimating the interference CM to design an adaptive filter, while the latter is used in estimating the scalar CFAR threshold for target detection. For non-homogeneous training conditions, however, N_{CFAR} is the number of *primary cell*s used for adaptive scalar CFAR detection; N_{CME} and N_{CFAR} cannot be traded-off against each other since both correspond to data sets containing different interferences [5, 6].

This paper continues our previous work [1]. In this paper, we propose a new adaptive detector in the framework of a two-stage adaptive detection structure [5, 6]. This structure provides a very simple solution for achieving the CFAR property in adaptive detectors employing the TMI filters suggested in [1]. The proposed detector combines scalar CFAR decisions from individual AMF detectors employing the LPMI and TMI filters to eliminate detection performance degradation resulting from possible SNR drop in TMI filters. This new detector is referred to as the two-stage joint loaded persymmetric-Toeplitz adaptive matched filter (TS JLPT-AMF) detector.

II. PROBLEM FORMULATION

In two-stage adaptive detectors, the required number of samples for adaptive CFAR control N_{CFAR} is independent of the antenna dimension M. For a sufficiently large array dimension M, therefore, any adaptive array filter requiring significantly smaller training sample support to achieve more efficient interference suppression than that required for the generic ML SCM estimator ($N_{3dB} \approx 2M$), will lead to a more efficient two-stage adaptive detector than any of the basic CFAR adaptive detectors [5, 6]. Thus, the superfast TMI filter introduced in [1] is the filter of choice for use in two-stage adaptive detectors. However, the TMI filters achieve a very high convergence rate ($N_{3dB} \approx m/2$) only if the angular separation between the interference sources is not too close to the SRL [2]. It should be noted that two-stage adaptive detection guarantees only strict CFAR control; it does not eliminate detection performance degradation due to a possible output SNR drop in TMI filters in scenarios with closely spaced sources.

Thus, this paper's primary task is to discover such a two-stage adaptive detector structure based on TMI filters that can ensure robust detection performance independently on angular separations between interferers.

To analyze the TS JLPT-AMF detector performance, we consider a scenario with a Swerling I target embedded in the interference with CM $\mathbf{R}$ that meets the condition (1). Here, the primary sample $\mathbf{y}$ is modeled as

$$\mathbf{y} = \begin{cases} \mathbf{x}_o \sim \mathcal{CN}(M, \mathbf{0}, \mathbf{R}) & \text{for hypothesis } H_o \\ \mathbf{x}_o + a\,\mathbf{s}_t,\ a \sim \mathcal{CN}(0, p_t) & \text{for hypothesis } H_1 \end{cases}, \quad (2)$$

where $\mathbf{x}_o \in \mathbb{C}^{M\times 1}$ is the observed interference plus receiver noise-only data vector, $\mathbf{s}_t = \mathbf{s}(\theta_t)$ is the normalized ($\mathbf{s}_t^H\mathbf{s}_t = 1$) array-signal steering vector for a target from a given direction θ_t (θ denotes DOA), and a represents the target complex amplitude fluctuations which power is p_t.

III. ADAPTIVE DETECTORS UNDER STUDY

Following [5, 6], we specify the two-stage loaded AMF (TS LAMF) detector as

$$\frac{|\mathbf{w}_{LSMI}^H\mathbf{y}|^2}{\mathbf{w}_{LSMI}^H\hat{\mathbf{R}}_{CFAR}\mathbf{w}_{LSMI}} = \eta_{LAMF} \underset{H_o}{\overset{H_1}{\gtrless}} h \quad (3)$$

where h is the scalar CFAR threshold constant and

$$\mathbf{w}_{LSMI} = \hat{\mathbf{R}}_{CME}(\beta)^{-1}\mathbf{s}_t,\ \hat{\mathbf{R}}_{CME}(\beta) = \hat{\mathbf{R}}_{CME} + \beta\hat{p}_o\mathbf{I} \quad (4)$$

$$\hat{\mathbf{R}}_{CME} = N_{CME}^{-1}\sum_{k=1}^{N_{CME}}\mathbf{x}_k\mathbf{x}_k^H,\ \hat{\mathbf{R}}_{CFAR} = N_{CFAR}^{-1}\sum_{k=N_{CME}+1}^{N}\mathbf{x}_k\mathbf{x}_k^H \quad (5)$$

with $\mathbf{x}_i \sim \mathcal{CN}(M, \mathbf{0}, \mathbf{R})$, i = 1, 2, … , N being the IID samples having an M-variate zero-mean complex circular Gaussian distribution with common covariance $\mathbf{R}$; the superscript ^{H} denotes the Hermitian transposition.

In this paper, we also introduce the two-stage loaded persymmetric AMF (TS LPAMF) detector as

$$\frac{|\mathbf{v}_{LPMI}^H\mathbf{y}|^2}{\mathbf{v}_{LPMI}^H\hat{\mathbf{R}}_{CFAR}\mathbf{v}_{LPMI}} = \eta_{LPAMF} \underset{H_o}{\overset{H_1}{\gtrless}} h \quad (6)$$

where $\mathbf{v}_{LPMI} = \mathbf{U}_P^H\mathbf{w}_{LPMI}$, $\mathbf{w}_{LPMI} = \hat{\mathbf{R}}_{RPCME}(\beta)^{-1}\mathbf{s}_{Pt}$, $\mathbf{s}_{Pt} = \mathbf{U}_P\mathbf{s}_t$, with $\mathbf{U}_P$ being the unitary matrix given by

$$\mathbf{U}_{\mathrm{P}} = \frac{1}{\sqrt{2}} \begin{bmatrix} \mathbf{I}_2 & \mathbf{J}_2 \\ j\mathbf{I}_2 & -j\mathbf{J}_2 \end{bmatrix} \tag{7}$$

where $\mathbf{I}_2$ and $\mathbf{J}_2$ respectively, are the $M/2$-by-$M/2$ identity and exchange matrix (we consider only the even M case), and the matrix $\hat{\mathbf{R}}_{\mathrm{RPCME}}(\beta)$ is given by [1]

$$\hat{\mathbf{R}}_{\mathrm{RPCME}}(\beta) = \hat{\mathbf{R}}_{\mathrm{RPCME}} + \beta\,\hat{p}_{\mathrm{o}}\mathbf{I}, \quad \hat{\mathbf{R}}_{\mathrm{RPCME}} = \mathrm{Re}(\mathbf{U}_{\mathrm{P}}\,\hat{\mathbf{R}}_{\mathrm{CME}}\,\mathbf{U}_{\mathrm{P}}^{\mathrm{H}}); \tag{8}$$

moreover, the two-stage Toeplitz AMF (TS TAMF) detector as

$$\frac{|\,\mathbf{v}_{\mathrm{TMI}}^{\mathrm{H}}\mathbf{y}\,|^2}{\mathbf{v}_{\mathrm{TMI}}^{\mathrm{H}}\hat{\mathbf{R}}_{\mathrm{CFAR}}\,\mathbf{v}_{\mathrm{TMI}}} = \eta_{\mathrm{TAMF}} \underset{\mathrm{H_o}}{\overset{\mathrm{H_1}}{\gtrless}} h \tag{9}$$

where $\mathbf{v}_{\mathrm{TMI}} = \mathbf{U}_{\mathrm{T}}^{\mathrm{H}}\mathbf{w}_{\mathrm{TMI}}$, $\mathbf{w}_{\mathrm{TMI}} = \hat{\mathbf{R}}_{\mathrm{RTCME}}^{-1}\mathbf{s}_{\mathrm{Tt}}$, $\mathbf{s}_{\mathrm{Tt}} = \mathbf{U}_{\mathrm{T}}\mathbf{s}_{\mathrm{t}}$, with $\mathbf{U}_{\mathrm{T}}$ being the unitary matrix given by

$$\mathbf{U}_{\mathrm{T}} = \frac{1}{\sqrt{2}}\,[\mathbf{I} - j\mathbf{J}] \tag{10}$$

where $\mathbf{I}$ and $\mathbf{J}$ respectively, represent the identity and exchange matrix of dimension M, and the matrix $\hat{\mathbf{R}}_{\mathrm{RTCME}}$ is computed as

$$\hat{\mathbf{R}}_{\mathrm{RTCME}} = \mathrm{Re}(\mathbf{U}_{\mathrm{T}}\,\hat{\mathbf{R}}_{\mathrm{TCME}}\,\mathbf{U}_{\mathrm{T}}^{\mathrm{H}}), \tag{11}$$

where $\hat{\mathbf{R}}_{\mathrm{TCME}}$ is the Toeplitz CM estimate computed with N_{CME} training samples using a noniterative model-matched Toeplitz CM estimator from [1]. In formulas (4) and (8) above, β is the loading factor and $\hat{p}_{\mathrm{o}}$ is the noise power estimate.

The new TS JLPT-AMF detector is defined as an adaptive detector that combines the scalar CFAR decisions associated with the TS LPAMF detector (6) and with the TS TAMF detector (9) using the following rule

$$\text{if } \eta_{\mathrm{LPAMF}} \ge h_{\mathrm{i}} \text{ or } \eta_{\mathrm{TAMF}} \ge h_{\mathrm{i}} \text{ then } \mathrm{H_1} \text{ is true, otherwise } \mathrm{H_o} \text{ is true} \tag{12}$$

where h_{i} is the individual CFAR threshold associated with a given individual probability of false alarm P_{FAi}. It follows from (12) that the decision strategy adopted in the TS JLPT-AMF detector is to declare that the hypothesis $\mathrm{H_1}$ is true (the target is present) whenever at least one of the individual two-stage detectors decides that $\mathrm{H_1}$ be true.

Theorem. The detection probability of detector (12) *exceeds the maximum of the individual detection probabilities.*

Proof. The proof is omitted.

This theorem above establishes the self-adjustment property of the TS JLPT-AMF detector; for the detector (12), the overall detection probability P_{D} is automatically maintained at a level such that P_{D} value always exceeds the maximum of the individual detection probabilities. For this reason, if the angular separation between sources is far enough from the SRL, the overall detection performance of detector (12) is maintained at some level exceeding the individual detection probability of the TS TAMF detector. If the TS TAMF detector performance should degrade due to the presence of closely spaced sources, the detector (12) will automatically maintain the P_{D} value at some level exceeding the individual detection probability of the TS LPAMF detector that is not sensitive to the angular separation $\Delta\theta$ between the sources because it uses the LPMI filter, which is not sensitive to $\Delta\theta$ [1]. Detector (12) robustness to the angular separation between sources is ensured thereby.

Note that detector (12) also increases the overall probability of false alarm P_{FA}, i.e., $P_{\mathrm{FA}} > P_{\mathrm{FAi}}$. The upper bound for P_{FA} follows from the inequality $P_{\mathrm{FA}} \le 2P_{\mathrm{FAi}}$ that can easily be proven assuming the hypothesis $\mathrm{H_o}$ (no target) is true.

IV. Performance Analysis

This section analyzes receiver operating characteristics (ROCs) of the two-stage detectors presented in Section III. For this analysis, homogenous training conditions are assumed when the full set of $N = 2M$ secondary IID training samples allocated for any single primary cell is divided into two subsets of size N_{CME} and N_{CFAR}, $N_{\mathrm{CME}}+N_{\mathrm{CFAR}} = N$.

In this analysis, we use the Root MUSIC-based TMI filter [1] in both of the TS TAMF detector and the TS JLPT-AMF detector. This TMI filter is designed using the Toeplitz CM estimator introduced in [1] with all the parameter settings specified therein. In comparative performance analysis, we also use the following benchmark detectors.

Benchmark detector 1 (BD1), BD1 is an optimal or clairvoyant detector achieving ultimate detection performance. This detector comprises the optimal Wiener filter $\mathbf{w}_{\mathrm{opt}} = \mathbf{R}^{-1}\mathbf{s}_{\mathrm{t}} / (\mathbf{s}_{\mathrm{t}}^{\mathrm{H}}\mathbf{R}^{-1}\mathbf{s}_{\mathrm{t}})$ followed by the decision rule

$$\frac{|\,\mathbf{y}^{\mathrm{H}}\mathbf{R}^{-1}\mathbf{s}_{\mathrm{t}}\,|^2}{\mathbf{s}_{\mathrm{t}}^{\mathrm{H}}\mathbf{R}^{-1}\mathbf{s}_{\mathrm{t}}} = \eta_{\mathrm{BD1}} \underset{\mathrm{H_o}}{\overset{\mathrm{H_1}}{\gtrless}} h\,. \tag{13}$$

The well-known expression describes the ROC curve of the detector (13)

$$P_{\mathrm{D}} = \exp[-|\ln P_{\mathrm{FA}}|/(1+q^2)], \tag{14}$$

where the output SNR of the optimal Wiener filter is

$$q^2 = p_{\mathrm{t}}\,\mathbf{s}_{\mathrm{t}}^{\mathrm{H}}\mathbf{R}^{-1}\mathbf{s}_{\mathrm{t}}\,. \tag{15}$$

The ultimate detection performance (14) corresponds to $N_{\mathrm{CME}} \to \infty$ and $N_{\mathrm{CFAR}} \to \infty$.

Benchmark detector 2 (BD2), BD2, a two-stage detector, comprises optimal Wiener filter and scalar cell averaging (CA) CFAR detector

$$\frac{|\,\mathbf{y}^{\mathrm{H}}\mathbf{R}^{-1}\mathbf{s}_{\mathrm{t}}\,|^2}{\mathbf{s}_{\mathrm{t}}^{\mathrm{H}}\mathbf{R}^{-1}\,\hat{\mathbf{R}}\,\mathbf{R}^{-1}\mathbf{s}_{\mathrm{t}}} = \eta_{\mathrm{BD2}} \underset{\mathrm{H_o}}{\overset{\mathrm{H_1}}{\gtrless}} h\,, \tag{16}$$

where $\hat{\mathbf{R}} = N^{-1}\sum_{k=1}^{N}\mathbf{x}_k\mathbf{x}_k^{\mathrm{H}}$ is the sample covariance matrix. Consequently, the detector (16) uses all N training samples for adaptive CFAR detection ($N_{\mathrm{CFAR}} = N$). The ROC of the detector (16) is given by

$$P_{\mathrm{D}} = \left[1 + h'/(1+q^2)\right]^{-N}, \tag{17}$$

where the modified CFAR constant $h' = h/N = P_{\mathrm{FA}}^{-1/N} - 1$. Equation (17) corresponds to $N_{\mathrm{CME}} \to \infty$ and $N_{\mathrm{CFAR}} = N$.

In all examples herein, a uniform linear array of $M = 12$ sensors, a Hamming weighted steering vector $\mathbf{s}_{\mathrm{t}}$ tuned to $\theta_{\mathrm{t}} = 0$ (providing a quiescent array pattern with –39 dB sidelobes), and the loading factor $\beta = 2$ for both the LSMI and the LPMI filters are used.

Fig. 1 compares the ROC of the TS JLPT-AMF detector with that of the TS TAMF detector, and with that of the TS LPAMF and the TS LAMF detectors in Scenario B specified in [1] as {$m = 4$, $\mathbf{u}$ =[–0.8, –0.4, 0.2, 0.5], **INR**(dB) = [20, 20, 20, 20]}, $\mathbf{u} = \sin(\boldsymbol{\theta})$, $\boldsymbol{\theta} = [\theta_1, \theta_2, \theta_3, \theta_4]$. The curves labeled "BD1" and "BD2" represent the ROCs for the corresponding benchmark detectors in the same scenario. One of the ROC

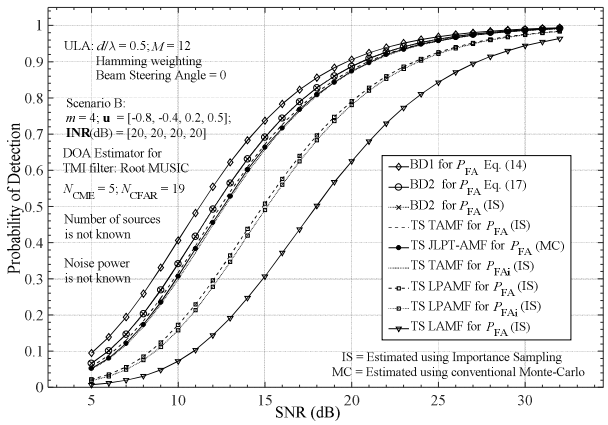

Fig. 1. ROCs for adaptive detectors under study; Scenario B, m is not known

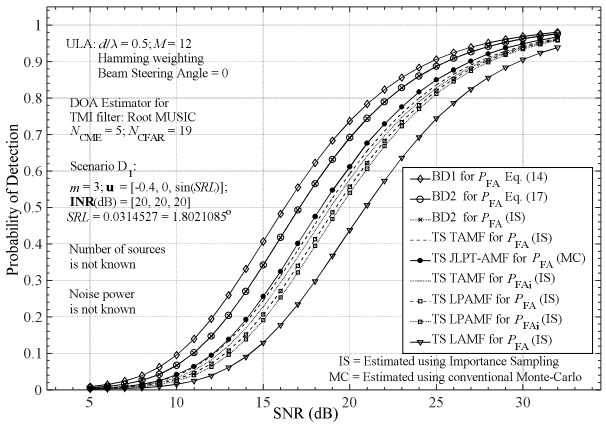

Fig. 2. ROCs for adaptive detectors under study; Scenario D_1, m is not known

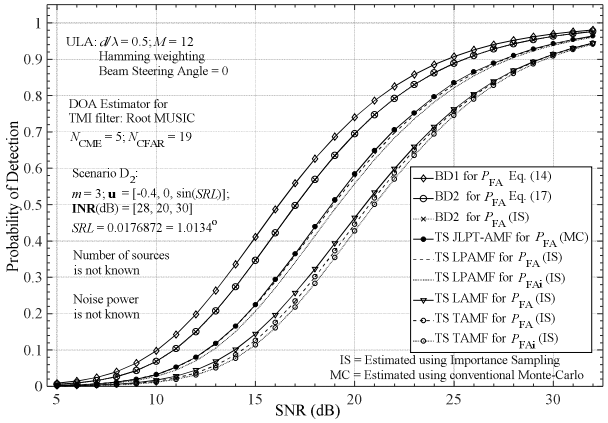

Fig. 3. ROCs for adaptive detectors under study; Scenario D_2, m is not known

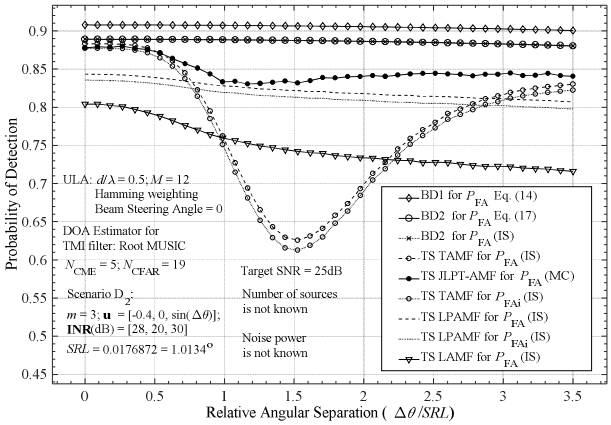

Fig. 4. Estimated probability of detection P_D versus $\Delta\theta/SRL$; Scenario D_2, m is not known

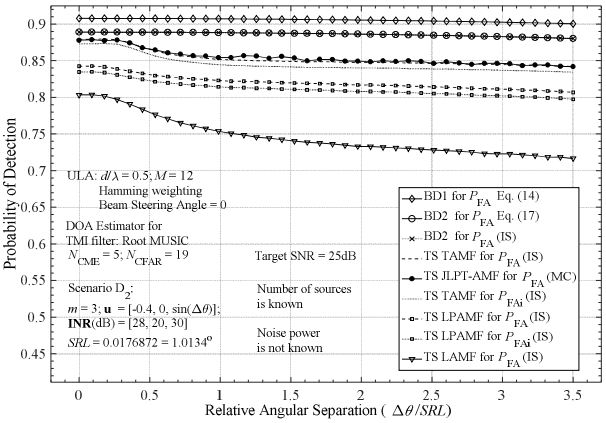

Fig. 5. Estimated probability of detection P_D versus $\Delta\theta/SRL$; Scenario D_2, m is known

curves for the BD2 is calculated for $P_{FA} = 10^{-4}$ from (17), and another is estimated using the Importance Sampling (IS) technique that employs a so-called g-method [10]. We developed two modified versions of the g-method: for estimating the probability of false alarm in case of arbitrary exact interference covariance matrix, and for estimating the detection performance for the target model specified in (2). The perfect match between these two ROC curves (between the analytic and estimated results) validates the high accuracy of the modified versions of the g-method: for $N_{IS} = 8{,}000$ independent statistical trials, the average relative standard deviation error is about 5% in estimating P_{FA} and about 1% in estimating P_D ($P_D \geq 0.3$).

Similarly, the ROC curves for the TS LAMF, the TS LPAMF, and the TS TAMF detectors are computed using the modified versions of the g-method, with $N_{IS} = 8{,}000$. In Fig. 1, two ROC plots, for $P_{FA}=10^{-4}$ and $P_{FAi}=0.671141\times10^{-4}$, are shown for each of the TS LPAMF and TS TAMF

detectors. Unfortunately, the g-method cannot be used for the TS JLPT-AMF detector; instead, we use the conventional Monte-Carlo (MC) technique with $N_{is} = 10^7$ to verify P_{FA} and with $N_{is} = 50{,}000$ to calculate the ROC curves.

In scenario B, the sources are sufficiently separated in the angular coordinate. By the sufficiently separated interference sources we understand the sources with such the smallest angular separation between them that is not too close to the SRL. In this paper, we define the SRL as

$$SRL = \frac{0.5\,FRL}{(SNR_{arr})^{1/4}} \tag{18}$$

where $FRL = 2\pi/M$ is the standard Fourier resolution limit and $SNR_{arr} = 4 \cdot M \cdot \mathrm{SNR}_{elt}$ is the array SNR with SNR_{elt} being the element-level SNR.

Fig. 1 shows that the TS JLPT-AMF detector exhibits superior detection performance in a scenario with sufficient angular separations between sources: for $P_D = 0.5$, the SNR gain relative to the TS LPAMF and the LAMF detectors is 2.3 dB and 5.4 dB, respectively, while the SNR loss relative to the unrealizable BD2 is just 0.5 dB.

Fig. 2 plots the ROCs for all the detectors being studied, and for the BD1 and BD2 detectors in Scenario $D_1 = \{m = 3$, $\mathbf{u} = [-0.4,\ 0.0,\ \sin(SRL)]$, **INR** (dB) = [20, 20, 20]} when the smallest angular separation between sources is equal to the statistical resolution limit $SRL = 1.80211^o$ (0.031457 rad) calculated from (18) for $SNR_{elt} = 20$ dB. Fig. 2 confirms the self-adjustment property of the TS JLPT-AMF detector. Indeed, the ROC curve for this detector goes above that for the TS TAMF detector; the latter represents the maximum of the two individual detection probabilities associated, respectively, with the TS LPAMF and the TS TAMF detectors at the specified individual probability of false alarm P_{FAi}.

Next, we consider an unfavorable scenario in which the convergence performance of the TMI filter may degrade [1]. Fig. 3 plots the ROC curves and Fig. 4 plots the estimated P_D versus the relative angular separation $\Delta\theta/SRL$ in Scenario D_2 $\{m = 3$, $\mathbf{u} = [-0.4,\ 0.0,\ \sin(SRL)]$, **INR** (dB) = [28, 20, 30]} when both p_o and m are not known. In this scenario, the statistical resolution limit $SRL = 1.0134^o$ (0.0176872 rad) for $SNR_{elt} = \max(\mathrm{INR}_2, \mathrm{INR}_3) = 30$dB. From Fig. 3, though the TS TAMF detector suffers essential performance degradation, for the TS JLPT-AMF detector, the ROC curve goes above that of the TS LPAMF detector at $P_{FAi} = 0.6711 \times 10^{-4}$ and slightly above that at $P_{FA} = 10^{-6}$. From Fig. 4, the TS TAMF detector collapses for $0.8SRL \le \Delta\theta \le 2.7SRL$, while for the TS JLPT-AMF detector, the P_D curve is above that of the TS LPAMF detector independently of the angular separation $\Delta\theta$. Figs. 3 and 4 confirm that the TS JLPT-AMF detector is robust.

In the same Scenario D_2, Fig. 5 plots the estimated P_D as a function of the relative angular separation $\Delta\theta/SRL$ under the assumption that m is known. Fig. 5 demonstrates that when the number of interference sources is known then the TS JLPT-AMF detector and the TS TAMF detector (both use the Root MUSIC-based TMI filter) are fundamentally robust to the angular separation.

V. Conclusion

In this paper, we have proposed new rapidly adaptive two-stage JLPT-AMF detectors that take advantage of superfast adaptive TMI filters based on a noniterative model-matched Toeplitz covariance matrix estimator introduced in [1]. These detectors possess two remarkable features. First, they exhibit reliable detection performances, which are robust to the angular separation between the interference sources, even when the training sample size to be used for estimating the interference covariance matrix is about $m/2 \sim m$ (m is the number of sources). This robustness has been analytically proven and verified with statistical simulations. Second, the two-stage JLPT-AMF detectors ensure the CFAR property independently of the antenna array dimension, the interference covariance matrix, and the number of training samples to be used for estimating this matrix.

For the first time, this paper has demonstrated that the necessary fundamental condition of reliable adaptive detection is determined by the ratio of the total number of real variables in a training data set to the total number of free real variables in the dominant eigenvectors of the exact covariance matrix. This ratio must exceed 2 to ensure reliable adaptive detection.

Finally, it is noteworthy that the denominator in (3), (6) and (9) can be rewritten as a sum of scalar samples, i.e., in the form that is specific for the conventional CA CFAR test [11, p. 215]. Having obtained scalar representations for the primary vector-samples assigned for CFAR thresholding, new scalar CFAR approaches [12, 13] can be used in severely nonhomogeneous environments to provide significant improvements in both, false alarm regulation and detection performance.

References

[1] A.A. Kononov, C.H. Choi and D.H. Kim, "Superfast convergence rate in adaptive arrays," in Proc. of Intern. Conf. on Radar 2018, Brisbane, Australia, 27 – 30 August 2018.

[2] S.T. Smith, "Statistical resolution limits and the complexified Cramér-Rao bound," IEEE Trans. SP, vol. 53, no. 5, p. 1602, May 2005.

[3] A.J. Barabell, "Improving the resolution performance of eigenstructure-based direction-finding algorithms," in Proc. ICASSP, Boston, MA, pp. 336–339, 1983.

[4] R. Roy and T. Kailath, "ESPRIT-Estimation of signal parameters via rotational invariance techniques," IEEE Trans. ASSP, vol. 37, no. 7, pp. 984–995, July 1989.

[5] Y.I. Abramovich, B.A. Johnson, and N.K. Spencer, "Sample-deficient adaptive detection: Adaptive scalar thresholding versus CFAR detector performance," IEEE Trans. AES, vol. 46, no. 1, pp. 32–46, January 2010.

[6] Maio, A.D. and M.S. Greco (Eds.), Modern Radar Detection Theory, Ch. 6, pp. 239-257, SciTech Publishing, Edison, NJ, 2016.

[7] I.S. Reed, J.D. Mallett and L.E. Brennan, "Rapid convergence rate in adaptive arrays," IEEE Trans. AES, vol. 10, no. 6, pp. 853–863, November 1974.

[8] O. Cheremisin, "Efficiency of adaptive algorithms with regularized sample covariance matrix," Radio Eng. Electron. Phys., vol. 27, no. 10, pp. 69–77, 1982.

[9] C.H. Gierull, "Statistical analysis of the eigenvector projection method for adaptive spatial filtering of interference," IEE Proc.-Radar, Sonar Navig., vol. 144, No. 2, pp. 57-63, April 1997.

[10] R. Srinivasan and M. Rangaswamy, "Importance sampling for characterizing STAP detectors," IEEE Trans. AES, vol. 43, no. 1, pp. 273–285, January 2007.

[11] F. C. Robey, D.R. Fuhrmann, E.J. Kelly, and R. Nitzberg, "A CFAR adaptive matched filter detector," IEEE Trans. AES, vol. 28, no. 1, pp. 208–216, January 1992.

[12] A.A. Kononov, J.H. Kim, J.K. Kim, and G. Kim "A new class of adaptive CFAR methods for nonhomogeneous environments," Progress in Electromagnetics Research B, vol. 64, 145-170, 2015. http://www.jpier.org/pierb/pier.php?paper=15091603.

[13] A.A. Kononov and J. Kim "Efficient elimination of multiple-time-around detections in pulse-Doppler radar systems," Progress in Electromagnetics Research B, vol. 71, 55-76, 2016. http://www.jpier.org/pierb/pier.php?paper=16083003.